A comprehensive study of the use of temporal moments in time-resolved diffuse optical tomography: part I. Theoretical material

N. Ducros, L. HervÉ, A. da Silva, J.-M. Dinten, F. Peyrin

A comprehensive study of the use of temporal moments in time-resolved diffuse optical

tomography: part I. Theoretical material

A comprehensive study of the use of temporal moments in time-resolved diffuse optical tomography: part I. Theoretical material

Nicolas Ducros[1,2]**, Lionel Hervé**[1]**, Anabela Da Silva**[3]**, Jean-Marc Dinten**[1] **and Françoise Peyrin**[2]

[1] CEA, LETI, MINATEC, 17 rue des Martyrs, F-38054 Grenoble, France
[2] CREATIS, INSERM U 630; CNRS UMR 5220; Université de Lyon; INSA de Lyon;
bât. Blaise Pascal, F-69621 Villeurbanne Cedex, France
[3] Institut Fresnel, CNRS UMR 6133; Université Aix-Marseille; École Centrale Marseille;
Campus universitaire de Saint-Jérôme, F-13013 Marseille

E-mail: nicolas.ducros@cea.fr

Abstract

The problem of fluorescence diffuse optical tomography consists in localizing fluorescent markers from near-infrared light measurements. Among the different available acquisition modalities, the time-resolved modality is expected to provide measurements of richer information content. To extract this information, the moments of the time-resolved measurements are often considered. In this paper, a theoretical analysis of the moments of the forward problem in fluorescence diffuse optical tomography is proposed for the infinite medium geometry. The moments are expressed as a function of the source, detector and markers positions as well as the optical properties of the medium and markers. Here, for the first time, an analytical expression holding for any moments order is mathematically derived. In addition, analytical expressions of the mean, variance and covariance of the moments in the presence of noise are given. These expressions are used to demonstrate the increasing sensitivity of moments to noise. Finally, the newly derived expressions are illustrated by means of sensitivity maps. The physical interpretation of the analytical formulae in conjunction with their map representations could provide new insights into the analysis of the information content provided by moments.

(Some figures in this article are in colour only in the electronic version)

Nomenclature

Symbol	Meaning	Units/Definition
μ_a	Absorption coefficient	cm^{-1}
μ_s'	Reduced scattering coefficient	cm^{-1}
$D = 1/(3\mu_s')$	Diffusion constant	cm
$\gamma^\star = (\mu_a/D)^{1/2}$	Wave number	cm^{-1}
ν	Speed of light within the medium	cm ns^{-1}
$\nu^\star = 2\nu(\mu_a D)^{1/2}$	Mean speed of the detected photons	cm ns^{-1}
τ	Fluorescence lifetime	ns
η	Fluorescence quantum yield	[-]
G	Green's function for the diffusion equation	W cm^{-2}
$\mathcal{G}$	Green's function for the diffusion equation in infinite media	W cm^{-2}
u^F	FDOT signal	W cm^{-2}
u	DOT-like signal	W cm^{-2}
e	Fluorescence pulse response	ns^{-1}
$f * g$	Convolution of f and g	$\int_{-\infty}^{+\infty} f(t')g(t-t')\,dt'$
$\hat{f}$	Fourier transform of f	$\int_{-\infty}^{+\infty} f(t)\exp(-j\omega t)\,dt$
$m_k[f]$	kth order moment of f	$\int_0^\infty f(t)t^k\,dt$
$\mathbf{s}$	Source position	
$\mathbf{d}$	Detector position	
$\mathbf{r}_n$	nth marker position	
$\mathbb{N}$	Set of integers	
$\mathbb{N}^*$	Set of strictly positive integers	

1. Introduction

Near-infrared (NIR) imaging techniques mainly benefit from low tissue absorption. Since photons can propagate over several centimetres within biological tissues at NIR wavelengths, they can be used to explore the inner tissue structure (Yodh and Chance 1995). Diffuse optical tomography (DOT) makes use of this ability and provides three-dimensional (3D) maps of the optical properties (Boas *et al* 2001, Gibson *et al* 2005). By employing a set-up including a set of external light sources and light detectors, the local absorption and diffusion coefficients can be estimated by solving an inverse problem (Arridge 1999). The development of new NIR fluorescent markers has led to a novel imaging technique called fluorescence DOT (FDOT) or fluorescence molecular tomography (FMT) (Paithankar *et al* 1997, Soubret and Ntziachristos 2006, Hervé *et al* 2007). This technique is capable of determining the 3D local concentrations of fluorescent markers.

Classically, DOT and FDOT approaches can be broadly classified into three modalities:

- *Continuous wave* (CW). The excitation light is steady, and the attenuation of the detected intensity is considered as the measurement (Schmitz *et al* 2002).
- *Frequency domain* (FD). The amplitude of the excitation light is modulated at radio-frequencies, typically around 100 MHz. The phase and demodulation between the excitation and detection intensities are recorded as the two measurements (Yu *et al* 2003).

- *Time domain* (TD). Ultrashort excitation pulses with time width in the picosecond or femtosecond range are used. At the detection point, the whole time course of the distorted pulse response is recorded over a range of about 10 ns with a time step varying from few picoseconds to few hundreds of picoseconds (Schmidt *et al* 2000).

CW measurements contain in nature less information than FD and TD since only the continuous component of the signals is exploited. In the context of DOT, Arridge and Lionheart (1998) have demonstrated that simultaneous recovery of absorption and diffusion coefficients maps cannot be achieved using the CW approach, contrary to FD and TD approaches. Using the latter approaches also enables one to limit the number of necessary detection points compared to CW. For instance, in the context of FDOT, Hall *et al* (2004) have shown that a unique fluorescent inclusion can be resolved with a single measurement point in the TD. Moreover, FD and TD offer the potential of fluorescence reconstruction with lifetime discrimination (Kumar *et al* 2008). FD and TD approaches are theoretically equivalent since FD and TD measurements are related by a Fourier transform. Practically speaking, the FD measurements are performed for a few modulation frequencies limiting the information content. As a result, the TD approach *a priori* maximizes the amount of information that can be acquired from a single TD measurement point.

Classically the TD measurements are not used directly but reduced to few features resulting from the application of a transformation along the time axis. This treatment is twofold: (i) reducing the redundancy in the measurements and (ii) reducing the computation cost of the forward model to a more tractable level. The optimal choice of the measurement features, initiated by Schweiger and Arridge (1999), is still a matter of debate. Global features such as the Laplace transform of the TD signals (Gao *et al* 2006) or the temporal moments of the TD signals (Hillman *et al* 2001, Liebert *et al* 2003, 2004, Lam *et al* 2005, Bloch *et al* 2005, Laidevant *et al* 2007, Marjono *et al* 2008) have been investigated. Recently, local features have received much attention. Riley *et al* (2007) have found that the photon peak value and time offer some advantages over the temporal moments. The selection of photons in early time windows has been increasingly investigated. It has allowed for reconstructions with better resolutions than with the CW approach or with the selection of photons in later time windows (Niedre *et al* 2008, Leblond *et al* 2009). However, the moments approach is still widely used due to specific advantages. First, the moments of the Green's light propagation functions can be calculated iteratively with a computation cost several order lower than that of the TD functions (Arridge and Schweiger 1995). Second, the moments allow for a physical interpretation of the features in terms of the numbers of photons and mean time of flights, which is of high interest in the understanding of the problem. Third, in practical problems the instrument response function implies to perform a convolution/deconvolution operation that is greatly simplified when moments are considered (Liebert *et al* 2003). Fourth and last, a noise model on the moments can be derived analytically from the TD measurement noise model (Liebert *et al* 2003, Arridge *et al* 1995).

A large number of studies based on the temporal moments have been undertaken. However, to our knowledge, there has been no clear evaluation of the benefit of using higher order moments. Generally, the use of the moments is limited to the orders from 0 to 2 (Liebert *et al* 2003, 2004, Lam *et al* 2005). In some cases only the first order is considered (Hillman *et al* 2001, Laidevant *et al* 2007, Marjono *et al* 2008). In a preliminary work, we observed that the benefits of higher order moments were related to the optical and fluorescence properties (Ducros *et al* 2008b). However, the underlying physical explanation for this situation is not fully established yet. In this context, the determination and understanding of the situations for which higher order moments are of interest is highly desirable.

The purpose of this two-part paper is to establish the domain of interest of the higher orders by analysing the information content they provide. In particular, the benefit of using higher orders will be evaluated against several parameters of interest. Under the scope of this study is the influence of: (i) the optical properties of the medium, (ii) the fluorescence lifetime of the marker and (iii) the noise level. It is believed that this moment-based study may provide new insights into the understanding of the more general time-resolved measurements.

This paper deals with the theoretical aspects of the use of moments in FDOT. Note that if the diffusion constant changes are small enough, then the problem of absorption perturbation reconstruction in DOT can be seen as a particular case of FDOT. As detailed in section 2, the present study is restricted to media where the diffusion approximation holds. We consider an infinite and homogeneous medium injected with a distribution of local fluorescent markers. Although this is a simple geometry, it has been previously used in practical situations (Thompson *et al* 2005). Moreover, the infinite medium expressions being developed here can easily be extended to expressions holding for more complex geometries (semi infinite, slab or parallelepiped) by means of the method of images (Kienle 2005). In section 3, we provide, as exhaustively as possible, the theoretical material that is required to build the moment-based FDOT forward model. To the best of our knowledge, this is the first time that an analytical expression of the moments of the FDOT forward model holding for any order is derived. Our expression generalizes the three expressions of moments at orders 0, 1 and 2 previously published by Lam *et al* (2005). In section 4, we analyse how the noise present on the TD measurement corrupts the moments. This novel derivation arises from the single assumption that the TD measurement noise follows a Poisson statistic.

The theoretical material developed in this paper will be exploited to address the inverse problem in a companion paper.

2. Theoretical background

2.1. Light propagation

The propagation of light in a turbid medium has been extensively discussed (e.g. see Ishimaru (1977)). In the context of FDOT, the diffusion approximation is often considered to be accurate enough to model the propagation of light. Within this framework, the photon density ϕ (in W m^{-2}) satisfies the following partial derivative equation:

$$-\nabla \left[D(\mathbf{r}) \nabla \phi (\mathbf{r}, \mathbf{s}, t) \right] + \frac{1}{\nu} \frac{\partial}{\partial t} \phi (\mathbf{r}, \mathbf{s}, t) + \mu_a(\mathbf{r}) \phi (\mathbf{r}, \mathbf{s}, t) = S(\mathbf{r}, \mathbf{s}, t). \qquad (1)$$

Here, D (in cm) is the diffusion constant defined by $D = 1/(3\mu_s')$ as recommended by Pierrat *et al* (2006); μ_s' (in cm) is the reduced scattering coefficient; μ_a (in cm) is the absorption coefficient; and ν (in cm ns^{-1}) is the speed of light within the medium. In the following, $G_{\mathbf{r},\mathbf{s}}(t)$ denotes the Green's function of the propagation operator, i.e. the solutions of (1) for $S(\mathbf{r}, \mathbf{s}, t) = \delta(\mathbf{r} - \mathbf{s})\delta(t)$ considering appropriate boundary conditions. An overview of the boundary conditions classically associated with (1), namely the extrapolated boundary conditions and the partial current boundary conditions, can be found in the work of Haskell *et al* (1994).

2.2. FDOT forward model

Classically, FDOT is simplified to a three-step process that involves (i) the propagation of light at the excitation wavelength λ_x from the source to the fluorescent marker; (ii) fluorescence, which stands for the absorption of some excitation light and its conversion to light at a higher
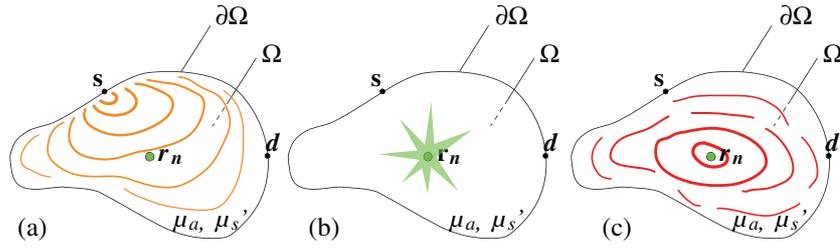
Figure 1. Basic schematic of the FDOT principle. (a) Excitation: the light emitted by the source at point **s** propagates through the medium. (b) Fluorescence: the fluorescent marker absorbs a part of the excitation light and re-emits a part of the absorbed light at a higher wavelength. (c) Emission: the light emitted by the fluorescent marker at point $\mathbf{r}_n$ propagates through the medium.

wavelength $\lambda_f > \lambda_x$; and (iii) the propagation of light at the fluorescence wavelength λ_f from the marker to the detector. This process, which neglects the re-absorption of fluorescence light by the fluorescent marker, is illustrated in figure 1.

Let us consider a fluorescent marker distribution $\{c_n\}_{n=1\ldots N}$, representing the local fluorescent marker concentrations at positions $\{\mathbf{r}_n\}_{n=1\ldots N}$. The fluorescence signal $u_{\mathbf{s},\mathbf{d}}(t)$ measured at detector position $\mathbf{d}$ after excitation at source position $\mathbf{s}$ is given by Patterson and Pogue (1994), Lam *et al* (2005):

$$u^F_{\mathbf{s},\mathbf{d}}(t) = \sum_{n=1}^{N} c_n \int_{-\infty}^{\infty} \int_{-\infty}^{\infty} G_{\mathbf{s},\mathbf{r}_n}(t'') e(t' - t'') G_{\mathbf{r}_n,\mathbf{d}}(t - t') \, \mathrm{d}t' \, \mathrm{d}t''. \tag{2}$$

To obtain a more concise expression, (2) is rewritten using the convolution operator $*$ defined in the nomenclature table. We obtain

$$u^F_{\mathbf{s},\mathbf{d}}(t) = \sum_{n=1}^{N} c_n \left(G_{\mathbf{s},\mathbf{r}_n} * e * G_{\mathbf{r}_n,\mathbf{d}} \right)(t), \tag{3}$$

where $e(t) = \eta \exp(-t/\tau)/\tau$ is the pulse response of the fluorescent marker that is parametrized by its fluorescence lifetime τ and quantum yield η. The functions $G_{\mathbf{s},\mathbf{r}_n}$ and $G_{\mathbf{r}_n,\mathbf{d}}$ denote the Green's functions of the propagation operator as defined in section 2.1. In (3), we use the classical assumption that the light acquisition set-up measures directly photon density. A more detailed discussion about this model can be found in Ducros *et al* (2008a).

It can be noted that $\exp(-t/\tau)/\tau$ tends to the Dirac's function when τ goes to 0. As a result, the special case ($\eta = 1$, $\tau = 0$) leads to

$$u_{\mathbf{s},\mathbf{d}}(t) = \sum_{n=1}^{N} c_n \left[G_{\mathbf{s},\mathbf{r}_n} * G_{\mathbf{r}_n,\mathbf{d}} \right](t). \tag{4}$$

One can recognize the right-hand side of (4) as the absorption kernel of the DOT problem (see equation (14) of Arridge (1995)). Thus, one can reinterpret $u_{\mathbf{s},\mathbf{d}}(t)$ as the light measured in the presence of the local absorption coefficient perturbation $\{\delta\mu_{a,n}\} = \{c_n\}$ neglecting the diffusion constant perturbation $\{\delta D_n\}$. This particular case of FDOT, for which the lifetime is set to 0 and the quantum yield to 1, will be referred to as the DOT-like case.

3. Derivation of the analytical expression of the higher order moments in an infinite medium

In this section, we consider an infinite medium that is classically associated with the vanishing boundary conditions: $\phi(\mathbf{r}, \mathbf{s}, t) \to 0$ when $\|\mathbf{r} - \mathbf{s}\| \to \infty$. In this context, our goal is to provide analytical formulae of the moments of the measured signals given in (3). Different definitions for the temporal moments have been employed in the past. Here, the following definition is adopted:

$$m_k[f] = \int_0^\infty f(t)t^k \, \mathrm{d}t, \qquad \forall\, k \in \mathbb{N}. \tag{5}$$

This definition has been chosen since it defines the moments as a linear transformation of the signal. Hence, this is the definition that allows for dealing with a linear inverse problem, which is done in the majority of FDOT cases. Moreover, such a definition allows for easily deriving the moments of a convolution (refer to appendix A).

The main results and starting point of this section is the novel derivation of (10) that gives the moments of a Green's function in an infinite medium for *any* order. All the succeeding formulations derive from this equation.

3.1. Moments of a Greens function for the diffusion equation

Let us introduce the two following parameters: $v^\star = 2v(\mu_a D)^{1/2}$ and $\gamma^\star = (\mu_a/D)^{1/2}$; $v^\star$ (in cm ns^{-1}) is referred to as the mean speed of the detected photons and $\gamma^\star$ (in cm) is referred to as the wave number. These two quantities appear naturally in the derivation of the moments. As will be discussed in section 5, these two parameters play a major role in the problem of FDOT.

The moments of a function can be advantageously expressed in the Fourier domain. Indeed, the kth-order moment of a function f is related to its Fourier transform $\hat{f}$ by (see equation (12) of Arridge and Schweiger (1995) for example)

$$m_k[f] = \mathrm{j}^k \frac{\mathrm{d}^k \hat{f}}{\mathrm{d}\omega^k}(\omega = 0). \tag{6}$$

For a homogeneous infinite medium, this approach is particularly suited to our problem since the Fourier transform of the Green's function for (1) is available. Interestingly, it only spatially depends on the propagation distance $l = \|\mathbf{r} - \mathbf{r_s}\|$ and is noted $\hat{\mathcal{G}}_l(\omega)$. Explicitly, $\hat{\mathcal{G}}_l(\omega)$ is given—after adaptation of equation (23) of Arridge *et al* (1992) to our notations—by

$$\hat{\mathcal{G}}_l(\omega) = \frac{1}{4\pi Dl} \exp[-x(\omega)^{1/2}], \qquad \text{with} \quad x(\omega) = 2\mathrm{j}\omega \frac{\gamma^\star}{v^\star} l^2 + (\gamma^\star l)^2. \tag{7}$$

Taking the kth derivatives of (7) leads to

$$\frac{\mathrm{d}^k \hat{\mathcal{G}}_l}{\mathrm{d}\omega^k} = \frac{1}{4\pi Dl} \left(\frac{\mathrm{j}l^2}{vD} \right)^k \frac{\mathrm{d}^k}{\mathrm{d}x^k} \exp(-x^{1/2}). \tag{8}$$

To go further, we use the lemma that is established below.

Lemma 1. *If $h(x) = \exp(-x^{1/2})$, then*

$$\frac{\mathrm{d}^k h}{\mathrm{d}x^k} = \frac{(-1)^k}{(2x)^k} \exp(-x^{1/2}) \sum_{p=1}^k \beta_p^k x^{p/2}, \qquad \forall\, k \in \mathbb{N}^* \tag{9a}$$

$$\text{where:} \quad \beta_p^k = \frac{2^p}{2^k} \frac{(2k - p - 1)!}{(k - p)!\,(p - 1)!} \tag{9b}$$

The use of lemma 1 in ([8](#)) and multiplication by j^k leads, after some algebra, to the following general formula:

$$m_k[\mathcal{G}_l] = \frac{1}{4\pi D}\frac{1}{l}\exp(-\gamma^\star l)\left(\frac{1}{\gamma^\star v^\star}\right)^k \mathcal{P}_k(\gamma^\star l), \qquad \forall\, k \in \mathbb{N}, \tag{10}$$

where $\mathcal{P}_k$ is a polynomial of order k, referred to as the reverse Bessel polynomial (Carlitz [1957](#)) and defined by

$$\mathcal{P}_k(x) = \begin{cases} 1, & \text{if} \quad k = 0 \\ \sum_{p=1}^{k} \beta_p^k\, x^p, & \forall\, k \in \mathbb{N}^*. \end{cases} \tag{11}$$

To illustrate the previous formula, the first four order moments are given as

$$m_0[\mathcal{G}_l] = \frac{1}{4\pi D}\frac{1}{l}\exp(-\gamma^\star l), \qquad m_2[\mathcal{G}_l] = m_0[\mathcal{G}_l]\left(\frac{1}{\gamma^\star v^\star}\right)^2 [\gamma^\star l + (\gamma^\star l)^2],$$

$$m_1[\mathcal{G}_l] = m_0[\mathcal{G}_l]\left(\frac{1}{\gamma^\star v^\star}\right)\gamma^\star l, \qquad m_3[\mathcal{G}_l] = m_0[\mathcal{G}_l]\left(\frac{1}{\gamma^\star v^\star}\right)^3 [3\gamma^\star l + 3(\gamma^\star l)^2 + (\gamma^\star l)^3].$$

$$\tag{12}$$

It is well known that the ratio $m_1[\mathcal{G}_l]/m_0[\mathcal{G}_l]$ represents the mean time of flight of the detected photons (Arridge *et al* [1992](#)). It can be observed that the mean time of flight is linearly related to the propagation distance l by $m_1[G]/m_0[G] = l/v^\star$. From this observation, it is natural to interpret $v^\star$ as the mean speed of the detected photons.

3.2. Moments of the convolution of two Green's functions

In an infinite homogeneous medium, the time convolution of two Green's functions can be expressed in terms of one single weighted Green's function. Denoting $l_{sn} = \|\mathbf{s} - \mathbf{r}_n\|$ and $l_{nd} = \|\mathbf{r}_n - \mathbf{d}\|$, we have

$$[\mathcal{G}_{l_{sn}} * \mathcal{G}_{l_{nd}}](t) = \frac{1}{4\pi D}\frac{l_{sn}+l_{nd}}{l_{sn}l_{nd}}\mathcal{G}_{l_{sn}+l_{nd}}(t). \tag{13}$$

This formula has been previously published in Hall *et al* ([2004](#)) and is demonstrated in appendix [C](#) for completeness. The moments of the convolution of two Green's functions readily derive from ([10](#)) and ([13](#)) and are given by

$$m_k[\mathcal{G}_{l_{sn}} * \mathcal{G}_{l_{nd}}] = \frac{1}{16\pi^2 D^2}\frac{1}{l_{sn}\,l_{nd}}\exp[-\gamma^\star(l_{sn}+l_{nd})]\left(\frac{1}{\gamma^\star v^\star}\right)^k \mathcal{P}_k[\gamma^\star(l_{sn}+l_{nd})], \quad \forall\, k \in \mathbb{N}. \tag{14}$$

3.3. Moments of the DOT-like forward model

To obtain the moments of the DOT-like measurement, the weighted sum of all contribution has to be considered as described by ([4](#)). Thanks to the linearity property of the moments (see ([A.1](#))), the following general expression is derived:

$$m_k[u_{\mathbf{s},\mathbf{d}}] = \frac{1}{16\pi^2 D^2}\left(\frac{1}{\gamma^\star v^\star}\right)^k \sum_{n=1}^{N} c_n \frac{1}{l_{sn}\,l_{nd}}\exp[-\gamma^\star(l_{sn}+l_{nd})]\mathcal{P}_k[\gamma^\star(l_{sn}+l_{nd})], \quad \forall\, k \in \mathbb{N}. \tag{15}$$

3.4. Moments of the fluorescence pulse response

Let $e(t)$ be the exponential decay of the fluorescence pulse response: $e(t) = \eta \exp(-t/\tau)/\tau$. It can be shown that the moments of $e(t)$ are given by

$$m_k[e] = \eta \, k! \tau^k, \qquad \forall \, k \in \mathbb{N}. \tag{16}$$

The demonstration of this formula is provided in appendix D.

3.5. Moments of the FDOT forward model

The FDOT moments $m_k\big[u_{s,d}^F\big]$ can be obtained as a function of the DOT-*like* moments of order 0 to k. Indeed, using the commutativity property of the convolution, it can be seen from (3) and (4) that

$$u_{s,d}^F(t) = [u_{s,d} * e](t). \tag{17}$$

Then, the convolution property of the moments given in (A.2) is applied onto the previous equation. We obtain

$$m_k\big[u_{s,d}^F\big] = \sum_{p=0}^{k} \binom{k}{p} \eta(k-p)! \tau^{k-p} \, m_p[u_{s,d}]. \tag{18}$$

It can be verified that the case $\tau = 0$ simplifies to $m_k\big[u_{s,d}^F\big] = m_k[u_{s,d}]$ as expected.

4. Derivation of the moment-based noise model

In this section, we restrict ourselves to the photonic noise that unavoidably corrupts light measurements. Indeed, this inherent Poisson noise arises from the stochastic nature of photon detection and is independent from the acquisition set-up. Here, the variance and covariance of the moments of TD measurements corrupted by a photonic noise are derived. Note that no hypothesis is made concerning the light propagation model or concerning the geometry of the media.

Let us start with the definition of the moments in which the integral is discretized. In practice, the TD signals are recorded over a finite time range $t \in [0, T]$ and sampled with a given time step ΔT. Let us consider the acquisition of Q samples and let N_q be the number of photons detected in the qth detection channel. Therefore, the kth-order moment is given by

$$m_k[f] = \int f(t)t^k \mathrm{d}t = \sum_{q=1}^{Q} N_q (q \, \Delta t)^k. \tag{19}$$

In real scenarios, the noiseless number of detected photons N_q is being perturbed by the presence of noise. To quantify the perturbation resulting on the moments, we adopt a statistical formalism. Let $\tilde{N}_q$ be some random variables describing the measured numbers of detected photons and $\tilde{m}_k$ be a random variable describing the measured kth-order moment. According to the Poisson noise assumption, we have $\mathrm{E}(\tilde{N}_q) = N_q$ and $\mathrm{var}(\tilde{N}_q) = \mathrm{E}(\tilde{N}_q)$. Moreover, the noise is supposed to be uncorrelated in time, i.e. the covariance between two distinct detection channels is zero. Under these assumptions, the mean and variance of the moments simplify to

$$\mathrm{E}(\tilde{m}_k) = \sum_{q=1}^{Q} \mathrm{E}(\tilde{N}_q)(q \, \Delta t)^k = m_k \tag{20}$$

and

$$\operatorname{var}(\tilde{m}_k) = \sum_{q=1}^{Q} \operatorname{var}(\tilde{N}_q)(q\,\Delta t)^{2k} = \sum_{q=1}^{Q} \operatorname{E}(\tilde{N}_q)(q\,\Delta t)^{2k} = \operatorname{E}(\tilde{m}_{2k}) = m_{2k}, \qquad (21)$$

where m_k stands for the noiseless kth-order moment.

Note that if the noiseless number of detected photons N_q is larger enough, then the Poisson distributed random variable $\tilde{N}_q$ can be modelled to a good approximation by a Gaussian distribution. In this case, the random variable $\tilde{m}_k$ is a weighted sum of independent Gaussian distributions. Thus, $\tilde{m}_k$ is itself a Gaussian-distributed random variable whose mean and variance are given by (20) and (21).

The covariance between two different order moments can also be expressed through a simple expression. The expression generalizing the previous formula is

$$\operatorname{cov}(\tilde{m}_i, \tilde{m}_j) = \operatorname{E}(\tilde{m}_{i+j}) = m_{i+j}. \qquad (22)$$

The demonstration of (22) is provided in appendix E. It can be mentioned that (21) and (22) are in agreement with the statistical properties derived by Arridge *et al* (refer more specifically to equation (46) of Arridge and Schweiger (1995)).

It has often been observed that moments of increasing order are increasingly sensitive to noise. To state it mathematically, let us define the signal-to-noise ratio (SNR) of a moment of order k by $R_k = 10 \log[\operatorname{E}(\tilde{m}_k)^2/\operatorname{var}(\tilde{m}_k)] = 10 \log(m_k^2/m_{2k})$. In this definition the SNR is expressed in dB. Originally, we show that the SNR of the moments satisfies the often-observed inequality:

$$R_k > R_{k+1}, \qquad \forall\, k \in \mathbb{N}. \qquad (23)$$

The demonstration for this formula is given in appendix F.

5. Analysis of the information content of the higher order moments

This section aims at discussing the information content provided by the higher order moments. Our purpose is to bring out some general intuitions about the benefits of using higher order moments. Therefore, the present discussion is limited to the direct observation of the moments resulting from the presence of a single fluorescent marker. A more rigorous reconstruction-based analysis is provided in a companion paper.

5.1. Zero lifetime case

Figure 2 illustrates the so-called sensitivity maps for moments of order 0 to 3, the fluorescence lifetime being set to 0. On a sensitivity map the source and detector positions **s** and **d** are fixed. Here $\|\mathbf{s} - \mathbf{d}\| = 5$ cm. A sensitivity map represents the moment measured for a given source and detector positions, with respect to the marker position $\mathbf{r}_n$. More specifically, a sensitivity map is a representation of (15) for different marker positions $\mathbf{r}_n$ around the source and detector positions. Moments corresponding to marker positions closer that 0.5 cm to the source or to the detector are not represented since the diffusion approximation fails when such small distances are reached. In the forthcoming discussion, the information content of the moments is examined from the patterns of the sensitivity maps. Hence, the latter have been normalized to the same maximum value.

Regardless of the order, it can be seen that the further to the source the marker is—or to the detector due to the symmetry of the problem—the smaller the moments are. This exhibits the dramatic lack of FDOT sensitivity to the deeply embedded marker. However, a deeply embedded marker leads to relatively higher moments when higher orders are considered.
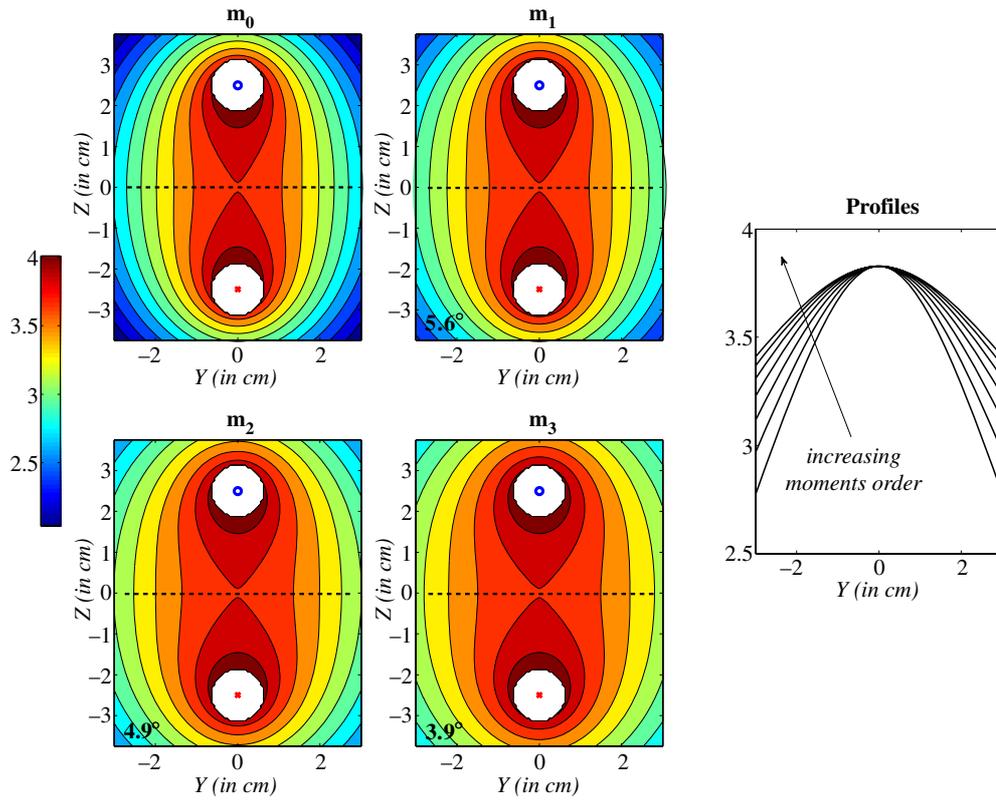
Figure 2. Sensitivity to the presence of a point-like fluorescent marker for different moment orders. The sensitivity is plotted with a log scale. On the right-hand side is plotted the sensitivity of the moments along the dash line of the left-hand side maps, for moment order from 0 to 6. The red cross indicates the source position and the blue circle the detector position. Optical properties: $\mu_a = 0.01$ cm^{-1}, $\mu_s' = 10$ cm^{-1} and $\tau = 0$ ns.

To understand the physical origin of the sensitivity patterns, let us inspect (15). Although this equation can seem complex, it takes the following simple form:

$$m_k(\mathbf{r}_n) = A_k \, m_0(\mathbf{r}_n) \, \mathcal{P}_k(\mathbf{r}_n), \tag{24}$$

where A_k is some constant depending on the optical properties of the medium and $\mathcal{P}_k$ is a polynomial of order k. To be more precise, $\mathcal{P}_k$ is a polynomial with respect to the propagation distance $l(\mathbf{r}_n) = \|\mathbf{s} - \mathbf{r}_n\| + \|\mathbf{r}_n - \mathbf{d}\|$. Note that the pattern of a m_k map does depend on the optical properties of the medium since both m_0 and $\mathcal{P}_k$ are functions of $\gamma^\star$ whereas it is not modified by $v^\star$ that only affects the multiplicative constant A_k. As a result, the information content of the moments are related to the optical properties of the medium through $\gamma^\star$. In terms of sensitivity maps, the simplified expression of m_k allows for interpreting a m_k sensitivity map as the results of a multiplication between a m_0 sensitivity map and a polynomial of order k map.

For the purpose of localizing a fluorescent marker, the more dissimilar at different moment orders the sensitivity maps are, the better it is. Indeed, two similarly patterned maps provide redundant information whereas maps with very different patterns indicate that complementary information is available. To quantify the similarity of the sensitivity maps—thus the amount
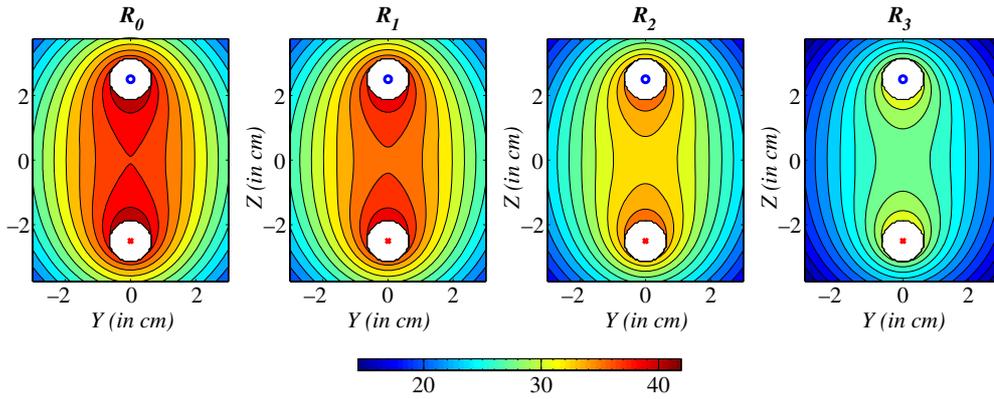
Figure 3. Signal-to-noise ratio maps. The red cross indicates the source position and the blue circle the detector position. Optical properties: $\mu_a = 0.01$ cm^{-1}, $\mu_s' = 10$ cm^{-1} and $\tau = 0$ ns. Figure 2.

of available information—the correlation between maps at different order has been evaluated. On the bottom left-hand corner of every m_k map (for $k \geqslant 1$), we report the corresponding correlation angle θ_k, which is the arccosine of the uncentred correlation between the current map m_k and the lower order map m_{k-1}. Specifically

$$\theta_k = \arccos\left(\frac{\mathbf{m_k} \cdot \mathbf{m_{k-1}}}{\|\mathbf{m_k}\| \|\mathbf{m_{k-1}}\|}\right), \qquad \text{where} \quad \mathbf{m_k} = [m_k(\mathbf{r}_1), \ldots, m_k(\mathbf{r}_n), \ldots, m_k(\mathbf{r}_N)]. \quad (25)$$

Within this geometrical framework, two fully correlated—equivalently proportional—maps satisfy $\theta = 0°$, while two uncorrelated maps satisfy $\theta = 90°$.

In our problem, the correlation between two moments of consecutive order is observed to be very strong since $\theta < 6°$ whatever the order. Moreover, the larger the order, the stronger the correlation. This suggests that the information content of the moments is getting poorer and poorer when the moments order is increased. This behaviour, in agreement with the increasingly close sensitivity profiles of figure 2, may be understood from the simplified expression of m_k given in (24). Indeed, this expression shows that the differences between two sensitivity patterns only originate from the $\mathcal{P}_k$ polynomials. Inspecting the coefficient of these polynomials, it can be seen that (i) they are all positive and (ii) they give relatively less and less weight to the monomial of order k than to the monomials of smaller orders for increasing k.

The two penalizing effects—the increase in the correlation of the moments and the increase in the noise sensitivity—should dramatically limit the practical use of higher order moments.

Figure 3 represents the SNR of moments for orders from 0 to 3. This representation showing the degradation of the SNR for higher orders is in agreement with (23). Moreover, it underlines the fact that the degradation of the SNR gets larger and larger when higher and higher orders are considered. This increasing sensitivity to noise is not linear with the moment order. While the SNRs of zeroth and first moments remain quite close, the SNRs of higher order moments experience stronger drops.

5.2. Non-zero lifetime case

In figure 4, the sensitivity maps for a fluorescent marker lifetime τ of 5 ns are represented. Comparing these maps to the maps depicted in figure 2 for which $\tau = 0$ ns, it can be seen that
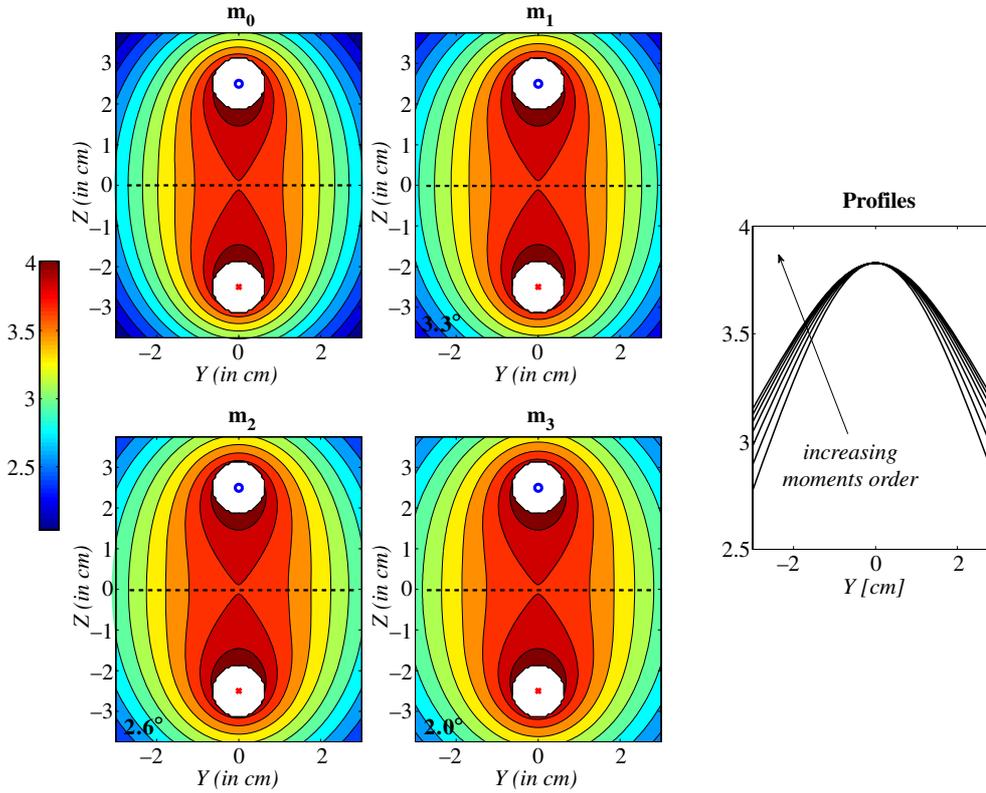
Figure 4. Sensitivity maps (log scale). The same conditions as in figure 2 but $\tau = 5$ ns.

increasing the marker lifetime from 0 to 5 ns results in a stronger correlation. To understand this phenomenon, let us inspect the effect of the fluorescence decay convolution as described by (18). For the first-order moment, it gives $m_1^F(\mathbf{r}_n) = \eta\tau m_0(\mathbf{r}_n) + \eta m_1(\mathbf{r}_n)$, which can be rewritten as $m_1^F(\mathbf{r}_n) = \eta m_0(\mathbf{r}_n)[\tau + A\mathcal{P}_1(\mathbf{r}_n)]$. Therefore, the first-order moment $m_1^F(\mathbf{r}_n)$ originates from two components: the first one related to the fluorescence itself, irrespective of the marker position, and the second one related to the marker position. If the lifetime τ is larger than $A\mathcal{P}_1(\mathbf{r}_n)$, then desirable part of the signal—the one depending on the marker position—is overwhelmed by the undesirable one—the one not depending on the marker position. As a result, it can be reasonably expected that the ability to determine the position of a fluorescent marker degrades for increasing τ. Furthermore, it can be readily noted that $A\mathcal{P}_1(\mathbf{r}_n) = l(\mathbf{r}_n)/v^\star$. Therefore, the amount of the desirable signal is smaller within a medium of high $v^\star$ than that within a medium of low $v^\star$. Hence, for a given τ, the ability to determine the position of a fluorescent marker should be improved with decreasing $v^\star$.

6. Conclusion

A theoretical study concerning the use of moments in TD FDOT has been proposed. Analytical expressions of the moments of the forward model of FDOT have been derived. Originally, these expressions for an infinite medium geometry hold whatever the moment order. The corruption of the moments due to the presence of noise on the time-resolved measurement has also been

studied, and simple expressions of the variance and covariance of the noise of the moments noise were derived. It was also proven that the SNR decreases with increasing moment orders. Then an analysis of the information content of the moments has been proposed. This analysis, based on the pattern of the sensitivity maps, has led to identify the following points:

  (i) the moments are strongly correlated,
 (ii) the moments of increasing order are increasingly correlated,
(iii) the moments of increasing order are increasingly more corrupted by noise,
(iv) the information content of the moments is related to the optical properties of the medium through parameter $\gamma^\star$ when the lifetime is zero,
 (v) the information content of the moments degrades when increasing lifetimes are considered,
(vi) for a given lifetime, the degradation of the information content of the moments depends on the optical properties of the medium through parameter $v^\star$.

In part II, the expressions derived here will be used in the resolution of the inverse problem allowing for recovering the 3D reconstructions of the markers concentrations. The influence of the SNR of the measurements as well as the optical properties of the medium and the fluorescence lifetime will be particularly investigated.

Acknowledgments

Appendix A. Properties of the moments

Assuming the moments are defined by $m_k[f] = \int f(t)t^k \, \mathrm{d}t$, the two following properties derive.

Property 1. *Linearity of the moments. Let the function f be the sum of the functions f_i. Thus, $f(t) = \sum_i f_i(t)$. The moments of f are related to the moments of f_i by the following formula:*

$$m_k[f] = \sum_i m_k[f_i], \qquad \forall \quad n \in \mathbb{N}. \tag{A.1}$$

Property 2. *Moments of a convolution. The moments of $f * h$ can be expressed in terms of the moments of f and h. Explicitly, it can be stated that*

$$m_k[f * h] = \sum_{p=0}^{k} \binom{k}{p} m_p[f] m_{k-p}[h], \qquad \forall k \in \mathbb{N}. \tag{A.2}$$

Appendix B. Proof of lemma 1

We write $h(x) = \exp(-x^{1/2})$ and want to show that the kth derivative of h satisfies (9).

First Step: By inspection of the first derivatives of h, it is observed that the general form of the kth derivative of h follows (9a). We assume that this formula holds up to order k, which is easily verified for $k = 1$.

Second Step: The $k + 1$th derivative of h is calculated by differentiation of (9a). After some algebra, this leads to

$$\frac{d^{k+1}h}{dx^{k+1}} = \frac{d}{dx}\frac{d^k h}{dx^k} = \frac{(-1)^{k+1}}{(2x)^{k+1}} \exp(-x^{1/2}) \sum_{p=1}^{k+1} \left[\beta_{p-1}^k + (2k - p)\beta_p^k\right] x^{p/2}. \tag{B.1}$$

This proves that the equality defined (9a) holds for any $k \in \mathbb{N}^*$. Moreover, the following relation between β_p^k is established: $\beta_p^{k+1} = \beta_{p-1}^k + (2k - p)\beta_p^k$. This relation generates the coefficients of the reverse Bessel polynomials whose explicit formula given in Sloane (2009) allows us to derive (9b) after some algebra. This concludes the proof of this lemma.

Appendix C. Moments of the convolution of two Green's functions of the diffusion equation

According to the convolution theorem, the Fourier transform of a convolution is the point-wise product of Fourier transforms. Thus, we consider the product $\hat{\mathcal{G}}_{l_1}(\omega)\hat{\mathcal{G}}_{l_2}(\omega)$. After substitution of the two Fourier transforms as given in (7), we have that

$$\hat{\mathcal{G}}_{l_1}(\omega)\hat{\mathcal{G}}_{l_2}(\omega) = \frac{1}{4\pi D l_1} \exp\left[-y(\omega)l_1\right] \frac{1}{4\pi D l_2} \exp\left[-y(\omega)l_2\right], \tag{C.1}$$

where $y(\omega) = \gamma^\star [2j\omega/(\gamma^\star v^\star) + 1]^{1/2}$. The terms are then rearranged to prove that

$$\hat{\mathcal{G}}_{l_1}(\omega)\hat{\mathcal{G}}_{l_2}(\omega) = \frac{1}{16\pi^2 D^2 l_1 l_2} \exp\left[-y(\omega)(l_1 + l_2)\right] = \frac{1}{4\pi D}\frac{l_1 + l_2}{l_1 l_2}\hat{\mathcal{G}}_{l_1+l_2}(\omega). \tag{C.2}$$

Appendix D. Moments of the fluorescence decay

We search for an analytic expression of the following integral:

$$m_k[e] = \frac{\eta}{\tau} \int_0^\infty \exp\left(-\frac{t}{\tau}\right) t^k \, dt. \tag{D.1}$$

Integrating (D.1) by parts, it can easily be shown that

$$m_k[e] = k\tau \, m_{k-1}[e], \qquad \forall \quad n \in \mathbb{N}^*. \tag{D.2}$$

By recursive use of the previous equality and with $m_0[e] = \eta$, we get that $m_k[e] = \eta k! \tau^k$.

Appendix E. Covariance of the noisy moments

Starting from the definition of the covariance of the two variables m_i and m_j we have to calculate

$$\text{cov}(\tilde{m}_i, \tilde{m}_j) = \text{E}(\tilde{m}_i\tilde{m}_j) - \text{E}(\tilde{m}_i)\text{E}(\tilde{m}_j). \tag{E.1}$$

First, we focus on the first term on the right-hand side of (E.1), replacing the moments by their discrete definition given in (19) and rearranging the different terms in order to obtain

$$\text{E}(\tilde{m}_i\tilde{m}_j) = \text{E}\left[\left(\sum_{q=1}^Q \tilde{N}_q (q\Delta t)^i\right)\left(\sum_{q'=1}^Q \tilde{N}_{q'}(q'\Delta t)^j\right)\right]$$

$$= \text{E}\left[\sum_{q=1}^Q \sum_{q'=1}^Q \tilde{N}_{q'}\tilde{N}_q (q\Delta t)^i (q'\Delta t)^j\right]. \tag{E.2}$$

Then, due to the linearity of expectation, we have that

$$\mathrm{E}(\tilde{m}_i \tilde{m}_j) = \sum_{q=1}^{Q} \sum_{q'=1}^{Q} \mathrm{E}(\tilde{N}_{q'} \tilde{N}_q)(q \Delta t)^i (q' \Delta t)^j. \tag{E.3}$$

Since the noise is assumed to be uncorrelated in time, $\tilde{N}_q$ and $\tilde{N}_{q'}$ are independent variables for all $q \neq q'$. Thus $\mathrm{E}(\tilde{N}_q \tilde{N}_{q'}) = \mathrm{E}(\tilde{N}_q)\mathrm{E}(\tilde{N}_{q'})$, $\forall q \neq q'$. However, the case $q = q'$ leads to $\mathrm{E}(\tilde{N}_q, \tilde{N}_q) = \mathrm{E}^2(\tilde{N}_q) + \mathrm{var}(\tilde{N}_q)$ since $\tilde{N}_q$ is obviously correlated to itself. Upon substitution of these two relations in (E.3), we have

$$\mathrm{E}(\tilde{m}_i \tilde{m}_j) = \sum_{q=1}^{Q} \mathrm{var}(\tilde{N}_q)(q \Delta t)^{i+j} + \sum_{q=1}^{Q} \sum_{q'=1}^{Q} \mathrm{E}[\tilde{N}_q]\mathrm{E}[\tilde{N}_{q'}](q \Delta t)^i (q' \Delta t)^j \tag{E.4}$$

$$= \sum_{q=1}^{Q} \mathrm{var}(\tilde{N}_q)(q \Delta t)^{i+j} + \mathrm{E}(\tilde{m}_i)\mathrm{E}(\tilde{m}_j). \tag{E.5}$$

With the Poisson statistic assumption stating that $\mathrm{var}(\tilde{N}_q) = \tilde{N}_q$ we finally obtain $\mathrm{cov}(\tilde{m}_i, \tilde{m}_j) = \mathrm{E}(m_{i+j})$.

Appendix F. The signal-to-noise ratio of the moments

To demonstrate (23), we generalize the problem and show that $\mathcal{R}(\kappa) = m_\kappa^2 / m_{2\kappa} = (\int f(t)t^\kappa \, \mathrm{d}t)^2 / \int f(t)t^{2\kappa} \, \mathrm{d}t$ is a decreasing function of the continuously defined variable κ. Therefore, we are to show that the derivative of $\mathcal{R}$ is negative for all κ.

First, the derivative $\mathcal{R}$ is derived and factorized as

$$\frac{\mathrm{d}\mathcal{R}}{\mathrm{d}\kappa}(\kappa) = 2A \left(\int f(t)\ln(t)t^\kappa \, \mathrm{d}t \int f(t)t^{2\kappa} \, \mathrm{d}t - \int f(t)\ln(t)t^{2\kappa} \, \mathrm{d}t \int f(t)t^\kappa \, \mathrm{d}t \right), \tag{F.1}$$

where $A = \int f(t)t^\kappa \, \mathrm{d}t / (\int f(t)t^{2\kappa} \, \mathrm{d}t)^2$ is positive since f is assumed to be positive.

Second, the two products of integrals are transformed into two double integrals, allowing for a new factorization. The integral transformation can be done in two equivalent manners:

$$\frac{\mathrm{d}\mathcal{R}}{\mathrm{d}\kappa}(\kappa) = 2A \iint f(u)f(v)[\ln(u)u^\kappa v^{2\kappa} - \ln(u)u^{2\kappa} v^\kappa] \, \mathrm{d}u \, \mathrm{d}v \tag{F.2a}$$

$$= 2A \iint f(u)f(v)[\ln(v)v^\kappa u^{2\kappa} - \ln(v)v^{2\kappa} u^\kappa] \, \mathrm{d}u \, \mathrm{d}v. \tag{F.2b}$$

Third, $\mathrm{d}\mathcal{R}/\mathrm{d}\kappa(\kappa)$ is written as the half-sum of (F.2a) and (F.2b), which permits a last factorization:

$$\frac{\mathrm{d}\mathcal{R}}{\mathrm{d}\kappa}(\kappa) = A \iint f(u)f(v)u^{3\kappa/2} v^{3\kappa/2} \ln\left(\frac{u}{v}\right) \left[\left(\frac{u}{v}\right)^{-\kappa/2} - \left(\frac{u}{v}\right)^{\kappa/2} \right] \mathrm{d}u \, \mathrm{d}v. \tag{F.3}$$

Noting that $\ln(x)(x^{-\epsilon} - x^\epsilon) < 0$, $\forall x > 0$ and $\epsilon > 0$ as well as $\ln(x)(x^{-\epsilon} - x^\epsilon) = 0$ if $\epsilon = 0$ concludes this demonstration.

References

Arridge S R 1995 Photon-measurement density functions: part I. Analytical forms *Appl. Opt.* **34** 7395
Arridge S R 1999 Optical tomography in medical imaging *Inverse Problems* **15** R41–93
Arridge S R, Cope M and Delpy D T 1992 The theoretical basis for the determination of optical pathlengths in tissue—temporal and frequency-analysis *Phys. Med. Biol.* **37** 1531–60

Arridge S R, Hiraoka M and Schweiger M 1995 Statistical basis for the determination of optical pathlength in tissue *Phys. Med. Biol.* **40** 1539

Arridge S R and Lionheart W R B 1998 Nonuniqueness in diffusion-based optical tomography *Opt. Lett.* **23** 882–4

Arridge S R and Schweiger M 1995 Direct calculation of the moments of the distribution of photon time of flight in tissue with a finite-element method *Appl. Opt.* **34** 2683

Bloch S, Lesage F, McIntosh L, Gandjbakhche A, Liang K X and Achilefu S 2005 Whole-body fluorescence lifetime imaging of a tumor-targeted near-infrared molecular probe in mice *J. Biomed. Opt.* **10** 054003

Boas D A, Brooks D H, Miller E L, DiMarzio C A, Kilmer M, Gaudette R J and Zhang Q 2001 Imaging the body with diffuse optical tomography *IEEE Signal Process. Mag.* **18** 57–75

Carlitz L 1957 A note on the bessel polynomials *Duke Math. J.* **24** 151–62

Ducros N, da Silva A, Dinten J-M and Peyrin F 2008a Approximations of the measurable quantity in diffuse optical problems: theoretical analysis of model deviations *J. Opt. Soc. Am.* A **25** 1174–80

Ducros N, Silva A D, Dinten J-M and Peyrin F 2008b Continuous wave and time-resolved fluorescence diffuse optical tomography: comparison for different lifetimes and optical properties *Biomedical Optics* (Washington, DC: Optical Society of America) p BMD25

Gao F, Zhao H J, Tanikawa Y and Yamada Y 2006 A linear, featured-data scheme for image reconstruction in time-domain fluorescence molecular tomography *Opt. Express* **14** 7109–24

Gibson A P, Hebden J C and Arridge S R 2005 Recent advances in diffuse optical imaging *Phys. Med. Biol.* **50** R1–43

Hall D, Ma G B, Lesage F and Yong W 2004 Simple time-domain optical method for estimating the depth and concentration of a fluorescent inclusion in a turbid medium *Opt. Express* **29** 2258–60

Haskell R C, Svaasand L O, Tsay T-T, Feng T-C, McAdams M S and Tromberg B J 1994 Boundary conditions for the diffusion equation in radiative transfer *J. Opt. Soc. Am.* A **11** 2727–41

Hervé L, Koenig A, Da Silva A, Berger M, Boutet J, Dinten J, Peltié P and Rizo P 2007 Noncontact fluorescence diffuse optical tomography of heterogeneous media *Appl. Opt.* **46** 4896–906

Hillman E M C, Hebden J C, Schweiger M, Dehghani H, Schmidt F E W, Delpy D T and Arridge S R 2001 Time resolved optical tomography of the human forearm *Phys. Med. Biol.* **46** 1117–30

Ishimaru A 1977 Theory and application of wave propagation and scattering in random media *Proc. IEEE* **65** 1030–61

Kienle A 2005 Light diffusion through a turbid parallelepiped *J. Opt. Soc. Am.* A **22** 1883–8

Kumar A T N, Raymond S B, Bacskai B J and Boas D A 2008 Comparison of frequency-domain and time-domain fluorescence lifetime tomography *Opt. Lett.* **33** 470–2

Laidevant A, Silva A D, Berger M, Boutet J, Dinten J-M and Boccara A C 2007 Analytical method for localizing a fluorescent inclusion in a turbid medium *Appl. Opt.* **46** 2131–7

Lam S, Lesage F and Intes X 2005 Time domain fluorescent diffuse optical tomography: analytical expressions *Opt. Express* **13** 2263–75

Leblond F, Dehghani H, Kepshire D and Pogue B W 2009 Early-photon fluorescence tomography: spatial resolution improvements and noise stability considerations *J. Opt. Soc. Am.* A **26** 1444–57

Liebert A, Wabnitz H, Grosenick D, Möller M, Macdonald R and Rinneberg H 2003 Evaluation of optical properties of highly scattering media by moments of distributions of times of flight of photons *Appl. Opt.* **42** 5785–92

Liebert A, Wabnitz H, Steinbrink J, Obrig H, Moller M, Macdonald R, Villringer A and Rinneberg H 2004 Time-resolved multidistance near-infrared spectroscopy of the adult head: intracerebral and extracerebral absorption changes from moments of distribution of times of flight of photons *Appl. Opt.* **43** 3037–47

Marjono A, Yano A, Okawa S, Gao F and Yamada Y 2008 Total light approach of time-domain fluorescence diffuse optical tomography *Opt. Express* **16** 15268–85

Niedre M J, de Kleine R H, Aikawa E, Kirsch D G, Weissleder R and Ntziachristos V 2008 Early photon tomography allows fluorescence detection of lung carcinomas and disease progression in mice *in vivo Proc. Natl Acad. Sci.* **105** 19126–31

Paithankar D Y, Chen A U, Pogue B W, Patterson M S and Sevick-Muraca E M 1997 Imaging of fluorescent yield and lifetime from multiply scattered light reemitted from random media *Appl. Opt.* **36** 2260–72

Patterson M S and Pogue B W 1994 Mathematical-model for time-resolved and frequency-domain fluorescence spectroscopy in biological tissue *Appl. Opt.* **33** 1963–74

Pierrat R, Greffet L J and Carminati R 2006 Photon diffusion coefficient in scattering and absorbing media *J. Opt. Soc. Am.* A **23** 1106–10

Riley J, Hassan M, Chernomordik V and Gandjbakhche A 2007 Choice of data types in time resolved fluorescence enhanced diffuse optical tomography *Med. Phys.* **34** 4890

Schmidt F E W, Fry M E, Hillman E M C, Hebden J C and Delpy D T 2000 A 32-channel time-resolved instrument for medical optical tomography *Rev. Sci. Instrum.* **71** 256–65

Schmitz C H, Löcker M, Lasker J M, Hielscher A H and Barbour R L 2002 Instrumentation for fast functional optical tomography *Rev. Sci. Instrum.* **73** 429–39

Schweiger M and Arridge S R 1999 Application of temporal filters to time resolved data in optical tomography *Phys. Med. Biol.* **44** 1699–717

Sloane N J A 2009 The On-line Encyclopedia of Integer Sequences—Sequences a001498 (published electronically)

Soubret A and Ntziachristos V 2006 Fluorescence molecular tomography in the presence of background fluorescence *Phys. Med. Biol.* **51** 3983–4001

Thompson M S, Johansson A, Johansson T, Andersson-Engels S, Svanberg S, Bendsoe N and Svanberg K 2005 Clinical system for interstitial photodynamic therapy with combined on-line dosimetry measurements *Appl. Opt.* **44** 4023–31

Yodh A and Chance B 1995 Spectroscopy and imaging with diffusing light *Phys. Today* **48** 34–40

Yu G, Durduran T, Furuya D, Greenberg J H and Yodh A G 2003 Frequency-domain multiplexing system for in vivo diffuse light measurements of rapid cerebral hemodynamics *Appl. Opt.* **42** 2931–9